FREE CONVECTION IN A VERTICAL CYLINDRICAL ANNULUS FILLED WITH ANISOTROPIC POROUS MEDIUM

by

Maruthu Rathinam THANSEKHAR, Inturi MAHESH BABU, and Ainavolu CHANDRA SEKHAR

Original scientific paper
UDC: 536.628:532.546:66.011
BIBLID: 0354-9836, *13* (2009), 1, 37-45
DOI: 10.2298/TSCI0901037T

A numerical study has been carried out for free convection in a vertical cylindrical annulus filled with a porous medium and whose inner wall is isothermally heated and the outer wall is isothermally cooled, the horizontal walls being insulated. The porous medium is assumed to be both hydrodynamically and thermally anisotropic. Numerical results are reported for 0.1 K^* 10, 0.1 λ 10, 1 A 20, 2 R_r 20, and Ra^* 10000. Anisotropy of the porous medium is found to affect fluid flow, temperature distribution and heat transfer significantly. Higher permeability in the vertical direction enhances convective flow intensity and heat transfer inside the annulus. Average Nusselt number on the inner hot wall increases with increase in Rayleigh number or radius ratio, while it decreases with increase in aspect ratio or permeability ratio. The influence of thermal anisotropy is not so significant as that of hydrodynamic anisotropy. The numerically predicted temperature distribution at various locations inside the annulus shows reasonable agreement with experimental results available for isotropic porous medium. Based on a parametric study, correlation for heat transfer is presented in terms of Rayleigh number, aspect ratio, radius ratio, and permeability ratio.

Key words: *anisotropy, permeability, Darcy, cylindrical annulus, free convection*

Introduction

In recent years there has been considerable advancement in the study of free convection in a porous annulus because of its natural occurrence and of its importance in many branches of science and engineering. This is of fundamental importance to a number of technological applications, such as under ground disposal of radioactive waste materials, cooling of nuclear fuel in shipping flasks and water filled storage bays, regenerative heat exchangers containing porous materials and petroleum reservoirs, burying of drums containing heat generating chemicals in the earth, storage of agricultural products, ground water flow modeling, nuclear reactor assembly, thermal energy storage tanks, insulation of gas cooled reactor vessels, high performance insulation for building, and cold storage. Free convective heat transfer inside a vertical annulus filled with isotropic porous medium has been studied by many researchers. Notable among them are Havstad *et al*. [1], Reda [2], Prasad *et al.* [3, 4], Prasad *et al*. [5], Hickox *et al.* [6], and Shivakumara *et al*. [7]. They concluded that radius ratio and Rayleigh number influence the heat and fluid flow significantly.

However, in many applications porous materials are anisotropic, such as columnar dendritic structures formed during solidification of multi-component mixtures, drying of preferentially oriented grains, tubular packed bed reactors, and rod bundle assemblies. Due to the preferential orientation of the porous matrix in the above applications the permeability and equivalent thermal conductivity of the porous matrix are different in different directions. The literature on anisotropic porous media is sparse in spite of its importance. Ni *et al*. [8] studied the effect of anisotropy of the porous medium inside a vertical enclosure. Free convection in a vertical cylinder filled with anisotropic porous medium has been studied by Chang *et al.* [9]. Parthiban *et al*. [10] studied onset of convection in a horizontal layer of heat generating anisotropic porous medium. Dhanasekaran *et al*. [11] analyzed the combined effect of heat generation and anisotropy inside vertical cylindrical enclosures. Three dimensional natural convection in anisotropic heat generating porous medium enclosed inside a rectangular cavity was studied by Suresh *et al*. [12]. From the review of literature, it is clear that effect of anisotropy of the porous medium inside a vertical cylindrical annulus has not been addressed yet. The objective of the present work is to analyze the effect of anisotropy of the porous medium on fluid flow and heat transfer inside a vertical cylindrical annulus.

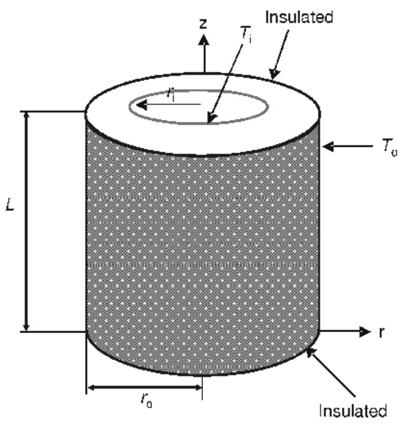

Figure 1. Physical configuration

Mathematical formulation

The physical configuration considered here is a vertical cylindrical annulus filled with anisotropic porous medium as shown in fig. 1. The inner and outer vertical walls of the annulus are maintained at constant temperatures T_i and T_o, respectively, where $T_i > T_o$. Both top and bottom boundaries are adiabatic. The porous matrix is anisotropic from both hydrodynamic and thermal point of view. The principal direction of permeability and thermal diffusivity are assumed to coincide with the horizontal (r) and vertical (z) co-ordinate axes (orthotropic porous medium). The convecting fluid and porous matrix are in local thermodynamic equilibrium. Darcy's law and Boussinesq approximation are valid. Darcy law is employed to represent the viscous term in the momentum equation. The governing equations for axi-symmetric steady flow through anisotropic porous medium are:

– continuity equation

$$\frac{\partial}{\partial r}(ru) \quad \frac{\partial}{\partial z}(rv) \quad 0 \tag{1}$$

– momentum equation

$$\frac{\partial p}{\partial r} \quad \frac{\mu}{K_r} u \quad 0 \tag{2}$$

$$\frac{\partial p}{\partial z} \quad \frac{\mu}{K_r} v \quad \rho g \beta (T \quad T_o) \quad 0 \tag{3}$$

– energy equation

$$u\frac{\partial T}{\partial r} \quad v\frac{\partial T}{\partial z} \quad \alpha_r \; \frac{1}{r}\frac{\partial}{\partial r} \quad r\frac{\partial T}{\partial r} \qquad \alpha_z \; \frac{\partial^2 T}{\partial z^2} \tag{4}$$

where K_r and K_z are permeabilities of the porous medium in radial (r) and axial (z) directions, respectively. α_r and α_z are thermal diffusivities along the r and z directions, respectively. The fluid velocities in the r and z directions present in the above equations are given as $u = -(1/r)(\;\psi'/\; z)$ and $v = (1/r)(\;\psi'/\; r)$. By employing the definition of stream function and eliminating the pressure terms from the momentum equations by cross differentiation, the governing eqs. (1)-(4) reduce to following the non-dimensional form as:

$$K^{*} A^{2}\gamma^{2} \frac{\partial}{\partial R} \quad \frac{1}{R}\frac{\partial\psi}{\partial R} \qquad \frac{\partial}{\partial Z} \quad \frac{1}{R}\frac{\partial\psi}{\partial Z} \qquad \mathrm{Ra}^{*} A\gamma \frac{\partial\theta}{\partial R} \tag{5}$$

$$\frac{\partial\psi}{\partial R}\frac{\partial\theta}{\partial Z} \quad \frac{\partial\psi}{\partial Z}\frac{\partial\theta}{\partial R} \quad \gamma \quad \frac{\partial}{\partial R} \quad R\frac{\partial\theta}{\partial R} \qquad \frac{1}{\lambda}\frac{1}{A^{2}\gamma} \quad \frac{\partial}{\partial Z} \quad R\frac{\partial\theta}{\partial Z} \tag{6}$$

The dimensionless variables used for writing the above equations are:

$$A \quad \frac{L}{D}, \; R_{\mathrm{r}} \quad \frac{r_{\mathrm{o}}}{r_{\mathrm{i}}}, \; \gamma \quad R_{r} \quad 1, \; Z \quad \frac{z}{L}, \; R \quad \frac{r}{r_{\mathrm{i}}}, \; \psi \quad \frac{D}{\alpha_{\mathrm{r}} r_{\mathrm{i}} L} \psi, \text{ and } \theta \quad \frac{T \quad T_{\mathrm{o}}}{\Delta T}$$

The relevant boundary conditions to solve the above equations are:

$$\psi = 0, \theta = 1 \text{ at } R = 1$$

$$\psi = 0, \theta = 0 \text{ at } R = R_{\mathrm{r}}$$

$$\psi = 0, \; \frac{\partial\Theta}{\partial Z} = 0 \text{ at } Z = 0 \text{ and } 1$$

Numerical method

The eqs. (5) and (6) are solved by finite volume method. A computer code, based on the finite volume method, is developed to solve the present problem. Central difference is used for discretizing all the terms except the convective term in the energy equation. For convective term, second upwind scheme has been employed. The algebraic equations thus obtained have been solved by the Gauss Seidel point-by-point solver, which makes use of the new values as soon as they are available.

Grid independence study

Various runs have been made to obtain the optimum grid size, which yields good accuracy and yet requires less computational time. A 81 81 mesh is found to be reasonably good for the Rayleigh number up to 5000 and 121 121 mesh was used for higher Rayleigh numbers. The code took longer time for convergence in the case of larger the values of aspect ratio, Rayleigh number or radius ratio.

Validation

In order to validate the computer code developed in this study, the problem of isotropic vertical annulus is studied by keeping $K^{*} = \lambda = 1$ in the code and the results are compared with those of Prasad *et al.*[3] as shown in tabs. 1 and 2; the results are for isotropic porous medium. It is observed that the present results are in good agreement.

Table 1. Comparison of average Nusselt number on the hot wall with the results of Prasad *et al.* [3]

	$A = 2$	$A = 4$			
Ra^{*} R_{r}	100 3	100 5	100 1.5	100 2	100 3
Prasad *et al.* [3]	4.738	5.716	2.751	3.123	3.692
Present results	4.632	5.74	2.7	3.096	3.666

Table 2. Comparison of average Nusselt number on the hot wall with the results of Prasad *et al.* [3]

	$R_r = 2$	$R_r = 5$	$R_r = 10$
Ra^*	50	120 80	135 90
A	10	2.5 12.5	5.55 1.111
Prasad *et al.* [3]	1.72	5.79 2.99	6.05 4.54
Present results	1.73	5.88 2.94	6.03 4.5

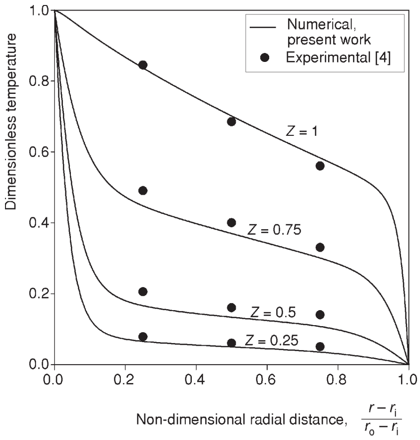

Figure 2. Comparison of predicted temperature distributions with the experimental results

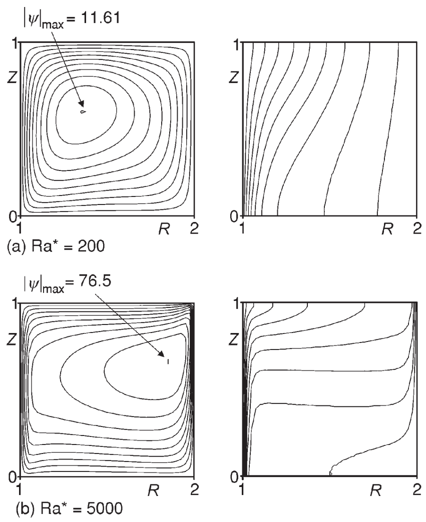

Figure 3. Effect of Rayleigh number on flow and temperature field for A = 1, R_r = 2, K^* = 1.0, and λ = 0.1

Comparisons with experimental results

The computer code is also validated against experimental work available in the open literature. The present work is compared with the experimental results carried out by Prasad *et al.* [4] for annulus filled with isotropic porous medium. The predicted temperature distributions inside the annulus at non-dimensional heights of Z = 0.25, 0.5, 0.75, and 1 are compared with the experimental data as seen in fig. 2. It can be observed that the agreement is good.

Results and discussions

Numerical results for a wide range of Rayleigh numbers Ra^* 10000, aspect ratios 1 A 20, radius ratios 2 R_r 20, permeability ratios 0.1 K^* 10, and thermal diffusivity ratios 0.1 λ 10 are reported.

Velocity and temperature fields

The flow pattern and temperature distribution are presented through plots of streamlines and isotherms. The rate of heat transfer is presented in terms of average Nusselt number on the inner hot wall. The flow consists of asymmetric single cell rotating in the clockwise direction *i. e.*, towards the cold wall. The fluid ascends along the inner hot wall and descends along the outer cold wall. In contrast to rectangular geometries, the convective cell is asymmetric about the vertical axis due to curvature effect (annular enclosure)

Effect of Rayleigh number

Figure 3 brings out the effect of Ra^* on streamlines and isotherms for unit aspect ratio and for different Rayleigh numbers. For Ra^* = 200, isotherms are almost vertical implying the conduction dominance. An increase in Rayleigh number shifts isotherms towards the inner hot wall. This results into a thinner thermal boundary layer on the hot wall and a thicker boundary layer on the cold wall. The isotherms in the core get stratified. A further increase in the Rayleigh number causes further stratification of the isotherms in the core. As Ra* increases the location of $|\psi|_{max}$ gets shifted towards the top right corner. The increase in $|\psi|_{max}$ indicating higher intensity of convection at higher Rayleigh numbers.

Effect of anisotropy

The effects of permeability ratio and thermal diffusivity ratio on the flow pattern and temperature distribution are shown in figs. 4 and 5. Figures 4(a-c) bring out the effect of hydrodynamic anisotropy through permeability ratio, K^*. Figure 4(b) illustrates the streamlines and isotherms for the isotropic case (*i. e.*, $K^* = \lambda = 1$). Figure 4(a) shows streamlines and isotherms for $K^* = 0.1$ (*i. e.*, the permeability in the vertical direction is higher than in the horizontal direction). There is an increase in maximum value of stream function indicating stronger convection. Sharp gradients in velocity and temperature are observed near the side walls. The core gets shifted towards the outer cold wall, resulting in higher convective velocities in the top right corner. As K^* decreases from 1 to 0.1 heat transfer rate increases as evident by closer spacing of isotherms near the side walls. Free convective flow along the side walls is much stronger for this case than for $K^* = 1.0$.

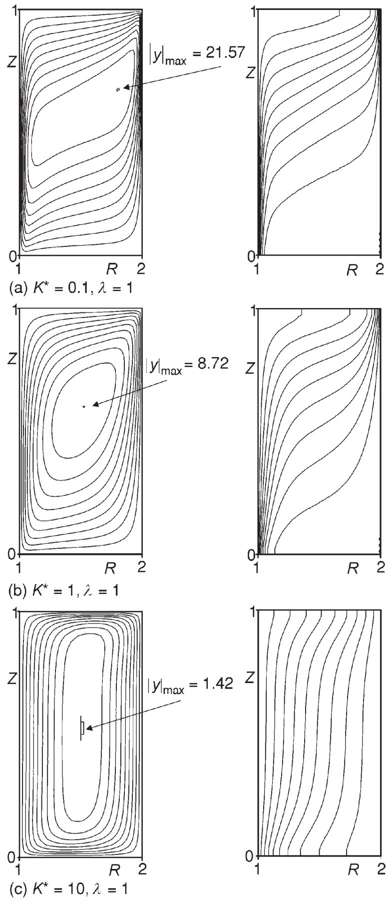

Figure 4. Effect of permeability ratio on flow and temperature field for A = 2, R_r = 2, Ra* = 200

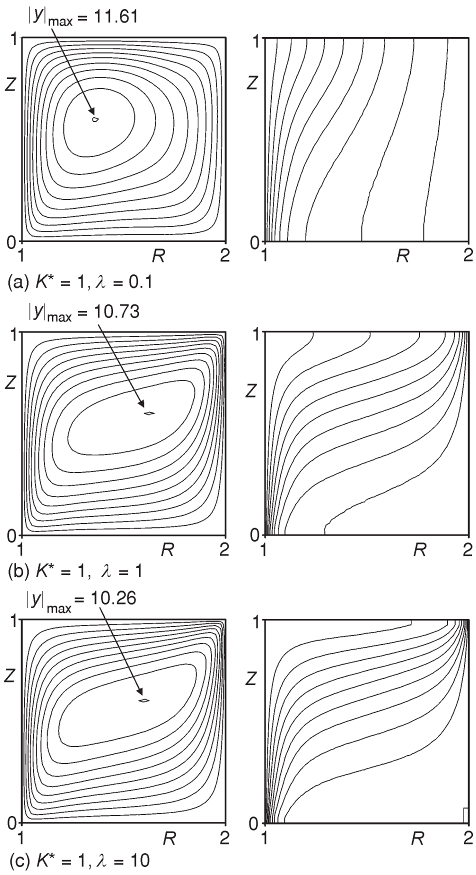

Figure 5. Effect of thermal diffusivity ratio on flow and temperature field, for A = 1, R_r = 2, Ra* = 200

The other extreme is shown in fig. 4(c). For $K^* = 10$, no sharp gradients in velocity and temperature are observed near the side walls, while the horizontally flowing fluid channels along the top and bottom adiabatic walls. This practically induces the so called "plug flow" in the fluid. The convective flow is weaker than the isotropic case, as seen by the reduction in the maximum value of stream function, due to the relatively lower permeability in the vertical direction. Consequently isotherms are almost vertical, indicating the conduction dominance.

Figure 5 shows the effect of thermal diffusivity ratio ($\lambda = \alpha_r/\alpha_z$) via streamlines and isotherms plots. Figure 5(b) depicts the flow and temperature patterns for isotropic case (*i. e.*, $K^* = \lambda = 1$). For $\lambda = 0.1$ – (see fig. (5a), the thermal diffusivity is much higher in the vertical direction than in the horizontal direction. Hence the temperature tends to be uniform in the vertical direction. As shown in figs. 5(b) and 5(c), for higher values of thermal diffusivity ratio, there is a slight shift in the isotherms towards the inner hot wall, while no appreciable change in the flow pattern is observed. It is observed that the effect of λ on flow intensity, as seen through the maximum stream function value, is not significant.

Temperature distribution at mid-height

The temperature distribution inside the annulus at mid-height ($Z = 0.5$) is shown in the fig. 6. Temperature drop near the inner hot wall is much more pronounced than that near the outer cold wall. Figure 6(a) illustrates the influence of permeability ratio (K^*) on the temperature distribution. For $K^* < 1$ (higher permeability in the vertical direction), the temperature gradient near the inner hot wall is steeper than that for $K^* > 1$, indicating better heat transfer, as also evident from fig. 4. As seen in fig. 6(b), the effect of λ on the temperature gradient near the inner hot wall is not so significant as that of K^*. However average temperature of the annulus increases with decrease in thermal diffusivity ratio, λ.

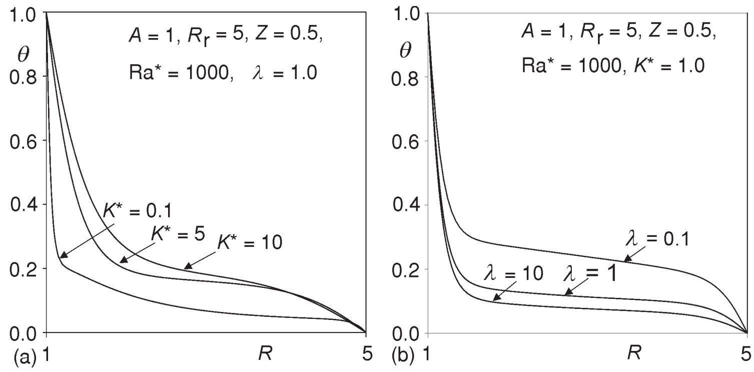

Figure 6. Temperature distribution at mid-height; (a) effect of permeability ratio; (b) effect of thermal diffusivity ratio

Heat transfer

The average Nusselt number on the inner (hot) wall is given, based upon the annulus gap width, D, as:

$$\overline{\mathrm{Nu}_\mathrm{i}} \quad \gamma_{1}^{R_\mathrm{r}} \; \frac{\partial\theta}{\partial R}_{R\;1} \, \mathrm{d}Z \qquad (7)$$

The heat transfer rates in terms of average Nusselt number on the inner wall are presented in figs. 7 and 8. Figure 7 illustrates the effect of hydrodynamic and thermal anisotropy (*i. e.* K^* and λ) of the porous medium on the average Nusselt number. The curves with darkened symbols show the variation of Nusselt number with permeability ratio (K^*). With increase in permeability ratio (*i. e.* lower permeability in the vertical direction), the Nusselt number decreases due to reduced flow intensity in the annulus as already observed in fig. 4(c). The curves with unfilled symbols refer to the variation of Nusselt number due to thermal diffusivity ratio (λ). The influence of λ on Nusselt number is not so significant.

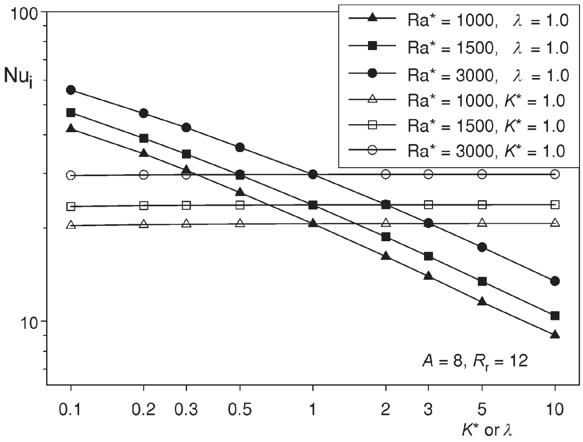

Figure 7. Variation of Nusselt number with permeability ratio and thermal diffusivity ratio

The effects of radius ratio and aspect ratio on average Nusselt number are depicted in fig. 8. The curves with unfilled symbols represent the variation of Nusselt number with aspect ratio. The Nusselt number is found to decrease with increase in aspect ratio of the annulus. The influence of radius ratio (R_r) of the annulus is shown by the curves with darkened symbols. With increase in radius ratio, the Nusselt number increases. However, for a given value of aspect ratio or radius ratio, an increase in Rayleigh number results in increase in Nusselt number as the Rayleigh number is the driving force for convective heat transfer.

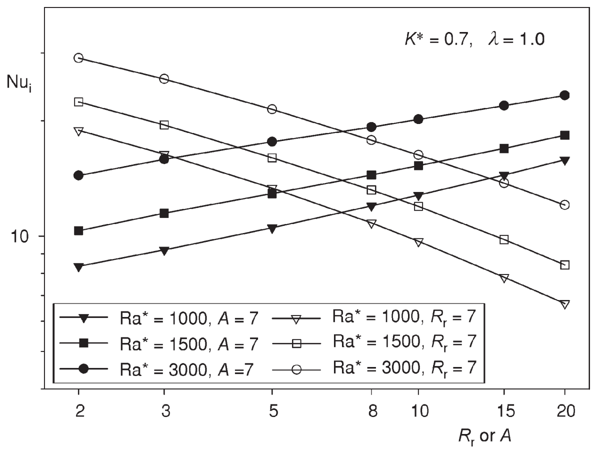

Figure 8. Variation of Nusselt number with aspect ratio and radius ratio

Correlations

Based upon the heat transfer results, the following correlation is presented for average Nusselt number on the inner hot wall in terms of Rayleigh number, radius ratio, aspect ratio, and permeability ratio:

$$\overline{\mathrm{Nu}}_{\mathrm{i}} \quad 1215\mathrm{Ra}^{*0.352} A^{\quad 0.294} R_{\mathrm{r}}^{0.191} K^{*\quad 0.256} \tag{8}$$

Equation (8) is valid for 0.5 K^* 5, 2 A 20, 2 R_r 20, and 500 Ra^* 10000. The thermal diffusivity ratio is not included as a parameter in developing the correlation as it has negligible effect on $\overline{\mathrm{Nu}}_{\mathrm{i}}$. The correlation agrees well with the data points, as seen from parity plot given in fig. 9. The correlation coefficient and the average percentage error of the correlation are 0.99 and 3.2, respectively, which shows the goodness of the fit.

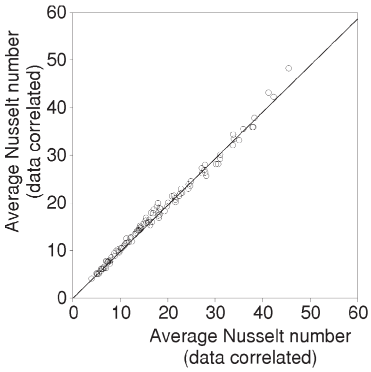

Figure 9. Comparison of $\overline{\mathrm{Nu}}_{\mathrm{i}}$ (data obtained) with $\overline{\mathrm{Nu}}_{\mathrm{i}}$ (correlated)

Conclusions

The effect of both hydrodynamic and thermal anisotropy, aspect ratio (A), radius ratio (R_r), and Rayleigh number (Ra*) inside a vertical cylindrical annulus filled with anisotropic porous medium is studied numerically. These parameters are found to influence the heat and fluid flow characteristics significantly. At low Rayleigh numbers conduction is significant where at high Rayleigh numbers convection dominates the total heat transfer. Higher permeability in the vertical direction causes higher flow intensity inside the annulus and steeper temperature gradients near the inner hot wall leading to better heat transfer. The thermal diffusivity ratio has only marginal effect on the flow intensity or heat transfer rate inside the annulus. The Nusselt number increases with increase in Rayleigh number or radius ratio whereas it decreases with increases in permeability ratio or aspect ratio. The effect of thermal diffusivity ratio on Nusselt number is not so significant for the entire range of parameters studied in the present work. Correlations for average Nusselt number on the inner hot wall have been proposed.

Nomenclature

A – aspect ratio (= L/D), [–]
D – gap width of porous annulus (= $r_o - r_i$), [m]
g – acceleration due to gravity, [ms^{-2}]
K – permeability, [m^2]
K^* – anisotropic permeability ratio (= K_r/K_z), [–]
L – height of the porous annulus, [m]
Nu – Nusselt number
P – pressure, [Pa]
Pr – Prandtl number (= ν/α –]
R – dimensionless distance in radial direction, (r/r_i), [–]
Ra* – Darcy modified Rayleigh number, (= $g\beta K_r D\Delta T/\nu\alpha_r$), [–]
R_r – radius ratio (= r_o/r_i), [–]
r – radial co-ordinate, [m]
T – temperature, [K]
ΔT – temperature difference (= $T_i - T_o$), [K]
u – fluid velocity in r-direction, [ms^{-1}]
v – fluid velocity in z-direction, [ms^{-1}]
Z – dimensionless distance in the axial direction (= z/L), [–]
z – axial co-ordinate, [m]

Greek letters

α – thermal diffusivity ratio, [m^{2}s^{-1}]
β – isobaric coefficient of thermal expansion of fluid, [K^{-1}]
γ – radius ratio parameter (= $D/r_i = R_r - 1$), [–]
λ – thermal diffusivity ratio (= α_r/α_z), [–]
θ – dimensionless temperature, [–]
μ – dynamic viscosity of the fluid, [Nsm^{-2}]
ν – kinematic viscosity of the fluid, [m^{2}s^{-1}]
ρ – fluid density, [kgm^{-3}]
ψ – dimensionless stream function (= $D/\alpha_r r_i L)\psi'$, [–]
ψ' – stream function, [m^{3}s^{-1}]

Subscripts

i – inner wall (heated)
o – outer wall (cooled)
r, z – radial and axial directions

References

[1] Havstad, M. A., Burns, P. J., Convective Heat Transfer in Vertical Cylindrical Annuli Filled with Porous Medium, *Int. J. Heat Mass Transf., 25* (1982), 11, pp. 1755-1766
[2] Reda, D. C., Natural Convection Experiments in a Liquid Saturated Porous Medium Bounded by Vertical Coaxial Cylinders, *ASME J. Heat Transfer, 105* (1983), 4, pp. 795-802
[3] Prasad, V., Kulacki, F. A., Natural Convection in a Vertical Porous Annulus, *Int. J. Heat Mass Transf., 27* (1984), 2, pp. 207-219

[4] Prasad, V., Kulacki, F. A., Natural Convection in Porous Media Bounded by Short Concentric Cylinders, *ASME J. Heat Transfer, 107* (1985), 1, pp. 147-154
[5] Prasad, V., Kulacki, F. A., Keyhani, M., Natural Convection in Porous Media, *J. Fluid Mechanics, 150* (1985), 3, pp. 89-119
[6] Hickox, C. E., Gartling, D. K., A Numerical Study of Natural Convection in a Vertical Annular Porous Layer, *Int. J. Heat Mass Transf., 28* (1985), 3, pp. 720-723
[7] Shivakumara, I. S., Prasanna, B. M .R., Rudraiah, N., Venkatachalappa, M., Numerical Study of Natural Convection in a Vertical Cylindrical Annulus Using a Non-Darcy Equation, *J. Porous Media, 5* (2003), 2, pp. 87-102
[8] Ni, J., Beckermann, C., Natural Convection in a Vertical Enclosure Filled with Anisotropic Porous Media, *ASME J. Heat Transfer, 113* (1991), 4, pp. 1033-1037
[9] Chang, W. J., Haiso, C. F., Natural Convection in a Vertical Cylinder Filled with Anisotropic Porous Media, *Int. J. Heat Mass Transf., 36* (1993), 5, pp. 3361-3367
[10] Parthiban, C., Patil, P. R., Thermal Instability in an Anisotropic Porous Medium with Internal Heat Source and Inclined Temperature Gradient, *Int. Commun. Heat Mass Transfer, 24* (1997), 7, pp. 1049-1058
[11] Dhanasekaran, M. R., Das Sarit, K., Venkateshan, S. P., Natural Convection in a Cylindrical Enclosure Filled with Heat Generating Anisotropic Porous Medium, *ASME J. Heat Transfer, 124* (2002), 1, pp. 203-207
[12] Suresh, Ch. S. Y., Vamsee Krishna, Y., Sundararajan, T., Das Sarit, K., Numerical Simulation of Three-Dimensional Natural Convection Inside a Heat Generating Anisotropic Porous Medium, *Heat Mass Transfer, 41* (2005), 9, pp. 799-809

Authors´ affiliations:

M. R. Thansekhar (**corresponding author**)
Dept. of Mechanical Engg.,
SSN College of Engg.,
Chennai, Tamil Nadu, India, Pin: 603 110
E-mail: thansekhar@yahoo.com, thansekhar@gmail.com

I. Mahesh Babu, A. Chandra Sekhar
M.E. (Computer Aided Design),
Dept. of Mechanical Engg.,
Sri Venkateswara college of Engg.
Pennalur, Sriperumbudur,
Tamil Nadu, India

Paper submitted: August 18, 2007
Paper revised: September 11, 2008
Paper accepted: December 8, 2008